

Supplementary Information

Hydrogen chloride (HCl) at ground sites during CalNex 2010 and insight into its thermodynamic properties

Ye Tao¹, Trevor C. VandenBoer¹, Patrick R. Veres², Carsten Warneke², Joost A. de Gouw^{3,4}, Rodney J. Weber⁵, Milos Z. Markovic^{6,7}, Yongjing Zhao⁸, Kirk R. Baker⁹, James T. Kelly⁹, Jennifer G. Murphy⁶, Cora J. Young¹, and James M. Roberts²

1. Department of Chemistry, York University, Toronto, Ontario, Canada
2. Chemical Sciences Laboratory, Earth System Research Laboratory, NOAA, Boulder, Colorado, USA.
3. Cooperative Institute for Research in the Environmental Sciences, University of Colorado, Boulder, Colorado, USA.
4. Department of Chemistry, University of Colorado Boulder, Boulder, Colorado, USA
5. School of Earth and Atmospheric Sciences, Georgia Institute of Technology, Atlanta, Georgia, USA
6. Department of Chemistry, University of Toronto, Toronto, Ontario, Canada.
7. now at Picarro Inc., Santa Clara, California, USA.
8. Air Quality Research Center, University of California, Davis, Davis, California, USA.
9. Office of Air Quality Planning and Standards, U.S. EPA, Research Triangle Park, North Carolina, USA.

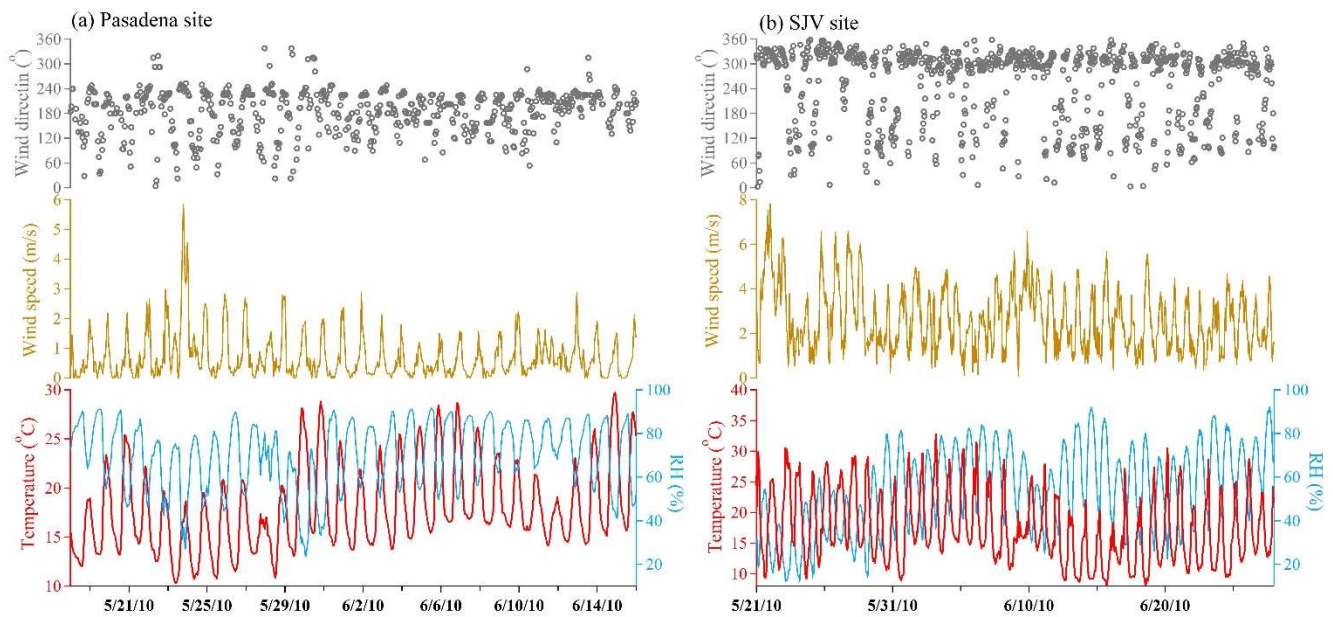


Figure S1. Meteorological parameters of 1-hour resolution including temperature, relative humidity, wind speed and wind direction at a) Pasadena and b) San Joaquin Valley (SJV) sites.

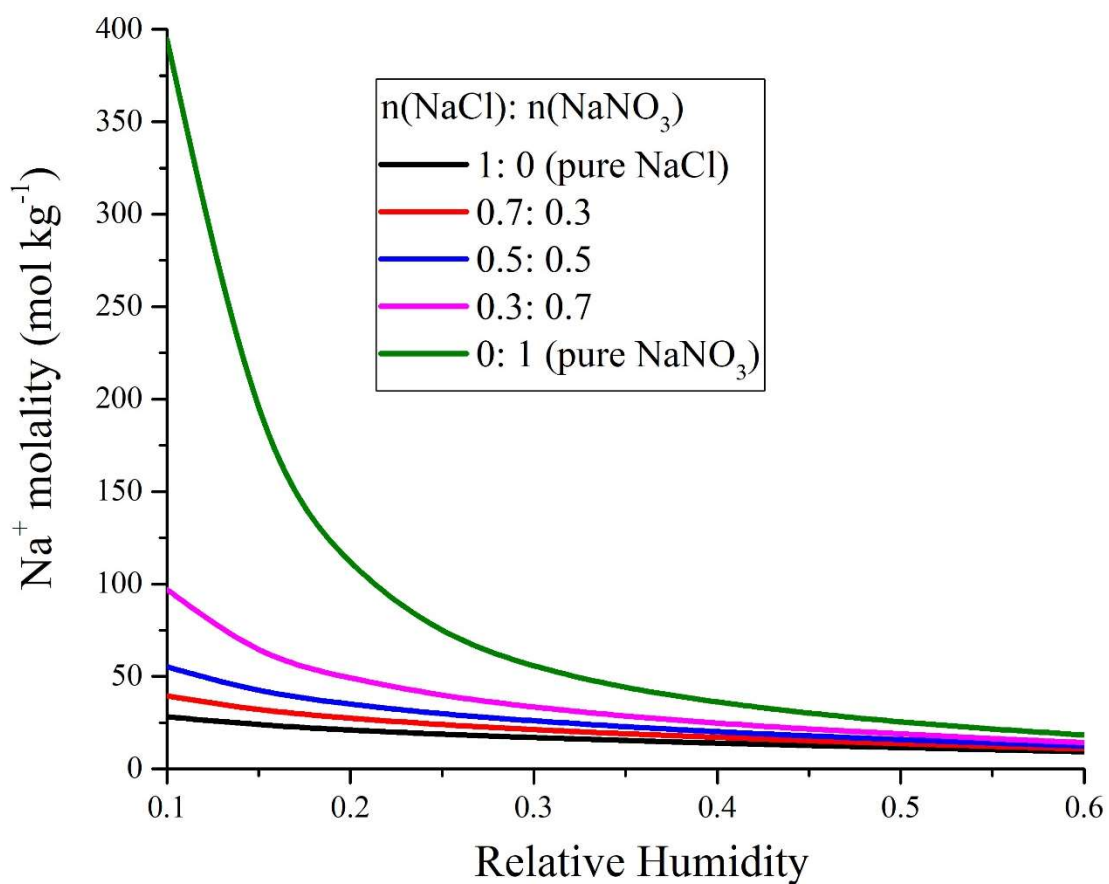


Figure S2. E-AIM III calculation results of Na^+ molality in metastable state particles as a function of RH under different molar ratios of $\text{NaCl}:\text{NaNO}_3$. Chloride-displacement reaction can significantly increase the Na^+ molality (also ionic strength) in aerosol liquid water in low RH conditions.

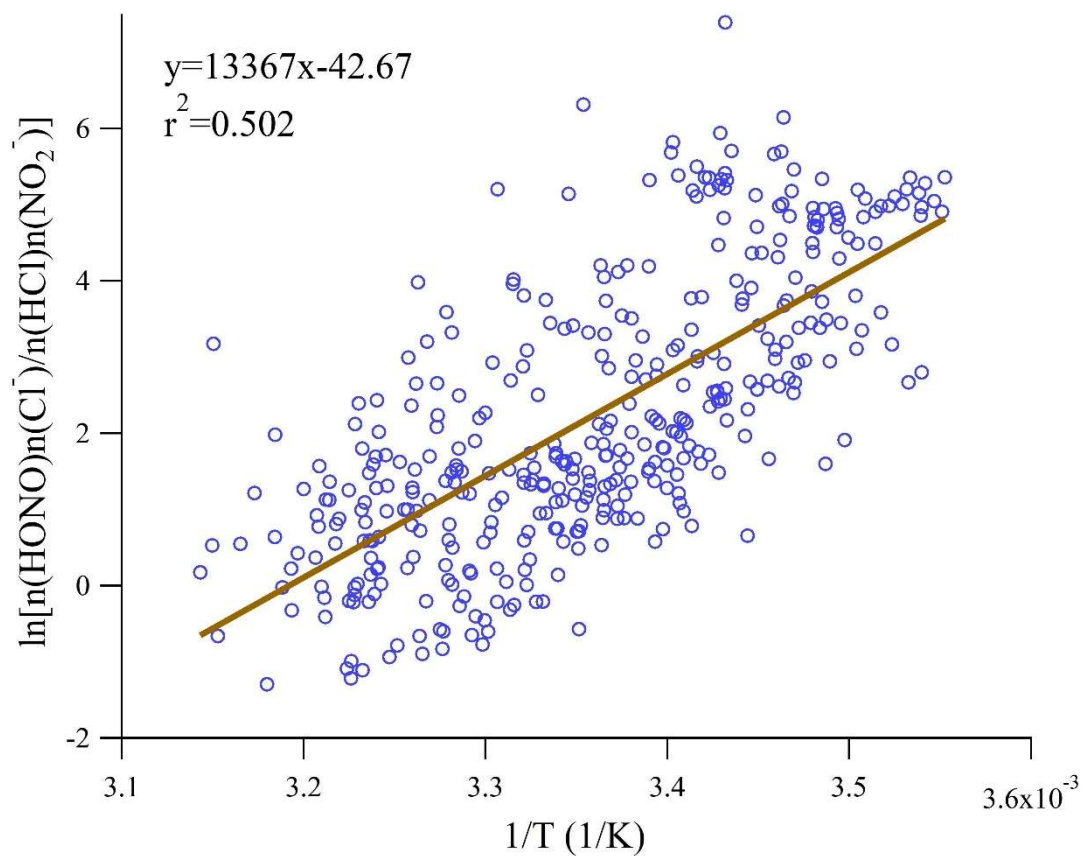


Figure S3. The linear regression of $\ln\left[\frac{n(\text{HONO})n(\text{Cl}^-)}{n(\text{HCl})n(\text{NO}_2^-)}\right]$ against $1/T$ in SJV site to study the coupled phase partitioning between HCl/Cl^- and $\text{HONO}/\text{NO}_2^-$.

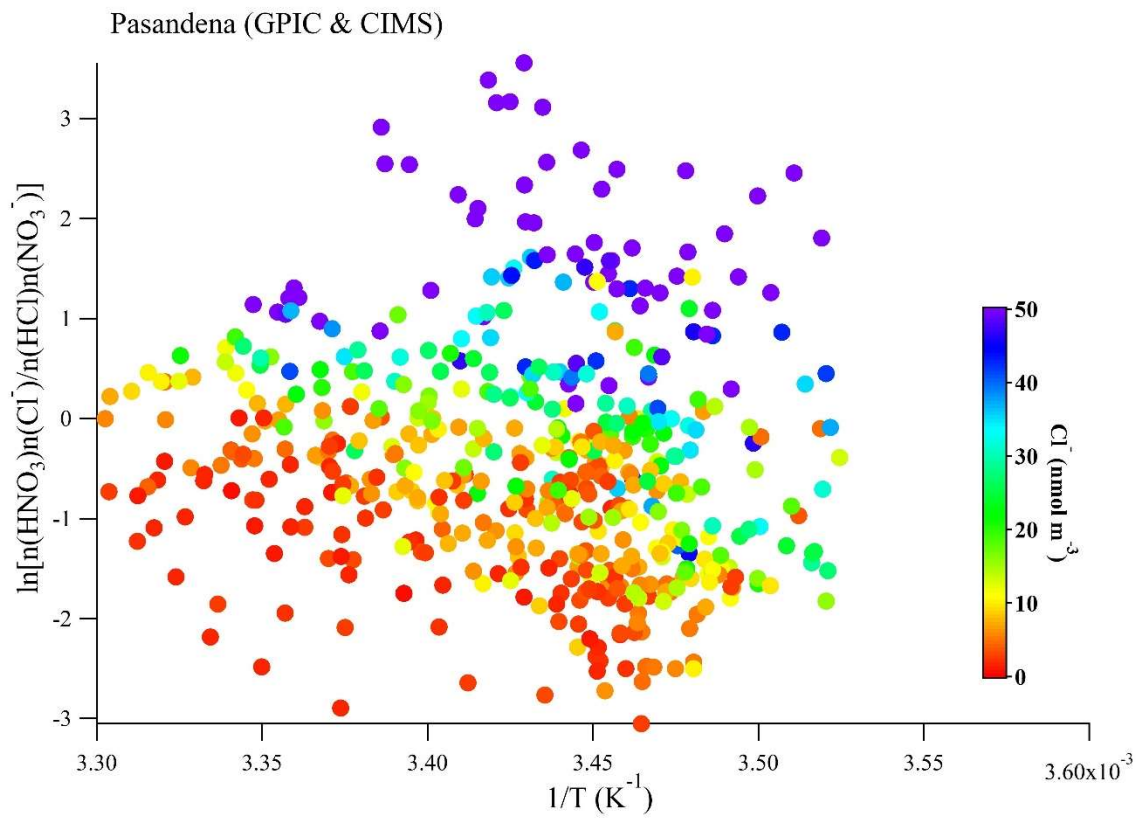


Figure S4. The plot of $\ln\left[\frac{n(\text{HNO}_3)n(\text{Cl}^-)}{n(\text{HCl})n(\text{NO}_3^-)}\right]$ against $1/T$ at Pasadena site.

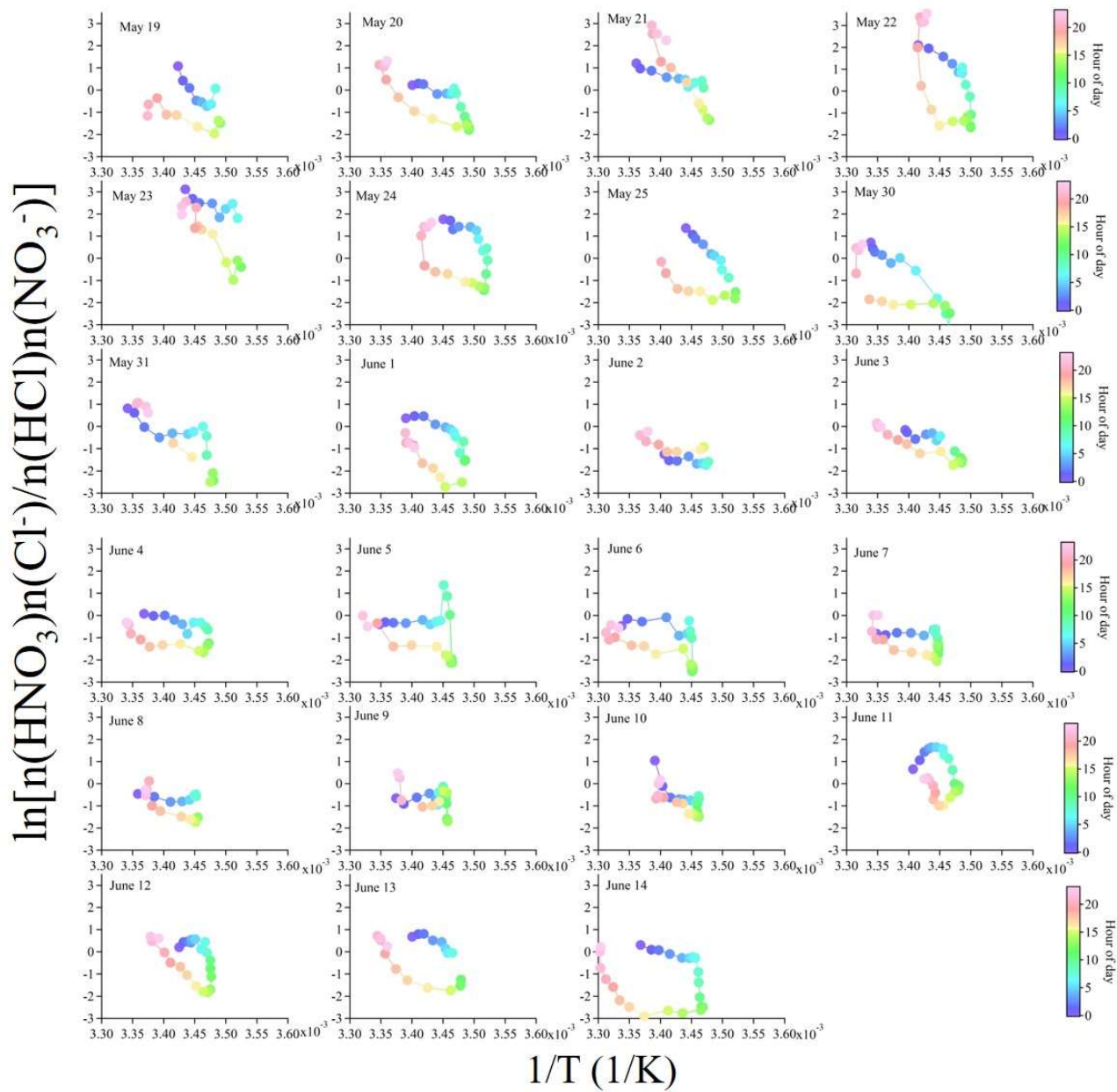


Figure S5. Day-by-day relationship between $\ln\left[\frac{n(\text{HNO}_3)n(\text{Cl}^-)}{n(\text{HCl})n(\text{NO}_3^-)}\right]$ and $1/T$ in Pasadena. Data points were colored by the hour of the day.

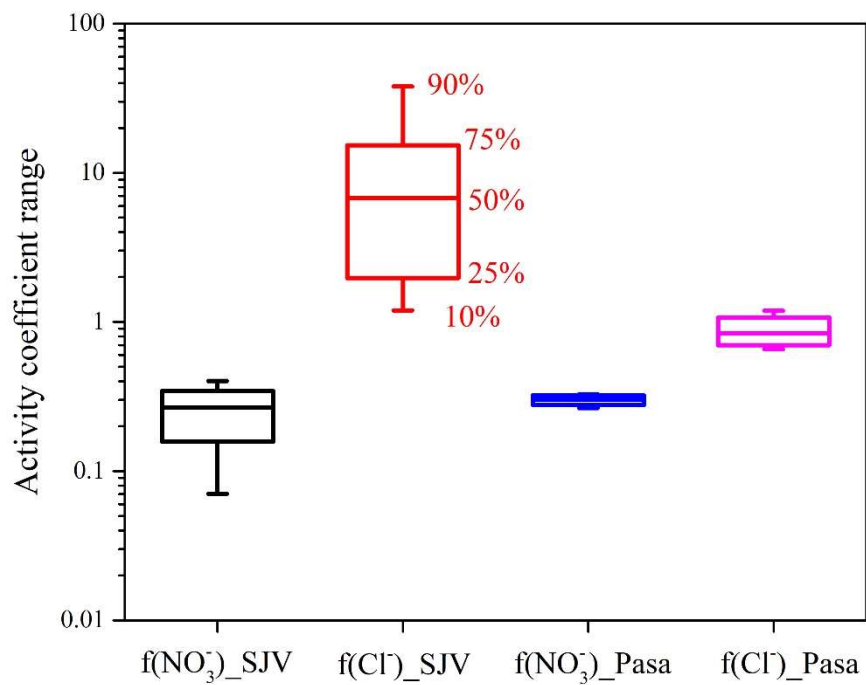


Figure S6. The activity coefficient range of particulate NO₃⁻ and Cl⁻ in SJV site and Pasadena site. The calculation was performed by E-AIM III for SJV site (due to low RH, temperature was set constant at 298.15 K) and E-AIM IV for Pasadena site.

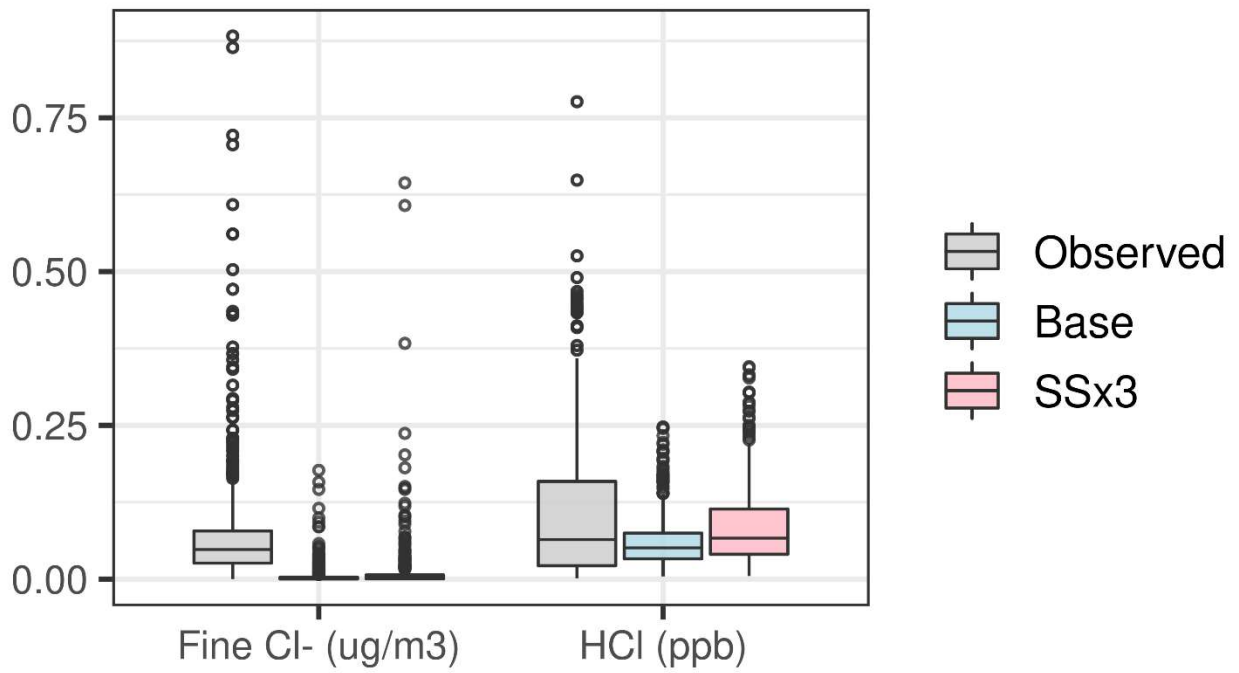


Figure S7. Modeled distributions of HCl and fine particulate Cl⁻ and at the SJV site. Circles represent values greater than 1.5 times the interquartile range from either end of the box.

Table S1. Summary of Effective Henry's Law Constant at 298K $K^0(298K)$ (atm^{-1}) and temperature dependence Δ_rH (kJ mol^{-1})

$\text{HNO}_3(\text{g}) \leftrightarrow \text{H}^+(\text{aq}) + \text{NO}_3^-(\text{aq})$		$\text{HCl}(\text{g}) \leftrightarrow \text{H}^+(\text{aq}) + \text{Cl}^-(\text{aq})$		$\text{HNO}_2(\text{g}) \leftrightarrow \text{H}^+(\text{aq}) + \text{NO}_2^-(\text{aq})$		Reference
$K^0(298K)$	Δ_rH	$K^0(298K)$	Δ_rH	$K^0(298K)$	Δ_rH	
853.1	-70.468	662.1	-72.561			[<i>Carslaw et al.</i> , 1995; <i>Clegg and Brimblecombe</i> , 1990]
814.9	-72.307	639.7	-74.860			[<i>Fountoukis and Nenes</i> , 2007]
786.7	-72.331	607~8.3 $\times 10^5$				[<i>Sander</i> , 2015; <i>Young et al.</i> , 2013]
		811.4	-43.299			[<i>Haskins et al.</i> , 2018]
1180.7	-73.014	658.8	-74.103	8.11 $\times 10^{-6}$	-29.272	[<i>Seinfeld and Pandis</i> , 2006]
		973~2369	-51.7~ -86.3			[<i>McGrath et al.</i> , 2013]
				8.6 $\times 10^{-7}$	-33.9	[<i>Rubio et al.</i> , 2009]
				8.04 $\times 10^{-6}$		[<i>Becker et al.</i> , 1998]
				8.42 $\times 10^{-6}$	-25.94	[<i>Park and Lee</i> , 1988]

Section 1: Semi-volatile NH₄Cl formation prediction:

An accurate description of HCl gas-particle equilibrium can be instructive in understanding the cycling of chlorine in the atmosphere and to the prediction of the magnitude and distribution of Cl⁻ available for activation, thereby impacting levels of photolabile reactive chlorine. The ammonia measurements that were made at both sites were used along with the HCl measurements to assess the extent to which formation of ammonium chloride (NH₄Cl) governs transport of HCl into the condensed phase as Cl⁻. Gas phase NH₃ and HCl are in equilibrium with fine mode particulate NH₄Cl (solid or aqueous) to an extent dependent on temperature and relative humidity [Meng and Seinfeld, 1996]. The product [NH₃][HCl] is depicted as a function of 1/T and RH, along with the equilibrium data reported by Pio and Harrison [1987], for the simplest case of pure NH₄Cl (Figure S8). In this plot, points that are below and to the left of the corresponding line for a given RH do not form a solid or droplet phase at equilibrium. At the Pasadena site, there was no NH₄Cl(s) predicted for RHs below deliquescence and NH₄Cl(aq) was predicted only when RH was above about 90% at the lowest temperatures from the campaign, i.e., at night and early morning at this surface site. As a consequence, NH₄Cl in aerosol represents a storage mechanism for soluble chloride only under cool damp conditions. At the SJV site, however, the dry conditions prevented any formation of NH₄Cl either as solid or aqueous aerosol. As a result, the measured condensed phase NH₄⁺ and Cl⁻ depends on other processes.

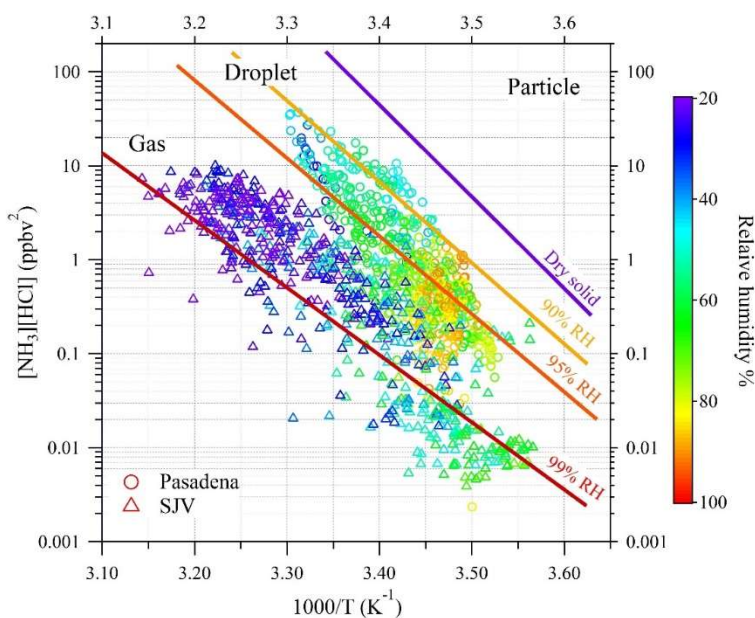


Figure S8. The product [NH₃][HCl] in ppbv² versus 1/T for the Pasadena data (circle) and SJV site (triangle) color coded by relative humidity. The colored lines correspond to the division between gas and condensed phases (either solid or droplet) for the RHs = 99%, 95%, 90% and dry conditions as given by Pio and Harrison [1987], respectively. Points above and to the right of the lines of their corresponding color indicate the presence of a condensed phase (either solid or droplet).

References:

- Becker, K. H., J. Kleffmann, R. Martin Negri, and P. Wiesen (1998), Solubility of nitrous acid (HONO) in ammonium sulfate solutions, *Journal of the Chemical Society, Faraday Transactions*, 94(11), 1583-1586.
- Carslaw, K. S., S. L. Clegg, and P. Brimblecombe (1995), A Thermodynamic Model of the System HCl-HNO₃-H₂SO₄-H₂O, Including Solubilities of HBr, from <200 to 328 K, *The Journal of Physical Chemistry*, 99(29), 11557-11574.
- Clegg, S. L., and P. Brimblecombe (1990), Equilibrium partial pressures and mean activity and osmotic coefficients of 0-100% nitric acid as a function of temperature, *The Journal of Physical Chemistry*, 94(13), 5369-5380.
- Fountoukis, C., and A. Nenes (2007), ISORROPIA II: a computationally efficient thermodynamic equilibrium model for K⁺-Ca²⁺-Mg²⁺-NH₄⁺-Na⁺-SO₄²⁻-NO₃⁻-Cl⁻-H₂O aerosols, *Atmospheric Chemistry and Physics*, 7(17), 4639-4659.
- Haskins, J. D., et al. (2018), Wintertime gas-particle partitioning and speciation of inorganic chlorine in the lower troposphere over the Northeast United States and coastal ocean, *Journal of Geophysical Research: Atmospheres*, 123(22).
- McGrath, M. J., I. F. Kuo, W. B. Ngouana, J. N. Ghogomu, C. J. Mundy, A. V. Marenich, C. J. Cramer, D. G. Truhlar, and J. I. Siepmann (2013), Calculation of the Gibbs free energy of solvation and dissociation of HCl in water via Monte Carlo simulations and continuum solvation models, *Phys Chem Chem Phys*, 15(32), 13578-13585.
- Meng, Z., and J. H. Seinfeld (1996), Time scales to achieve atmospheric gas-aerosol equilibrium for volatile species, *Atmospheric Environment*, 30(16), 2889-2900.
- Park, J. Y., and Y. N. Lee (1988), Solubility and decomposition kinetics of nitrous acid in aqueous solution, *The Journal of Physical Chemistry*, 92(22), 6294-6302.
- Pio, C. A., and R. M. Harrison (1987), Vapour pressure of ammonium chloride aerosol: Effect of temperature and humidity, *Atmospheric Environment (1967)*, 21(12), 2711-2715.
- Rubio, M. A., E. Lissi, G. Villena, Y. F. Elshorbany, J. Kleffmann, R. Kurtenbach, and P. Wiesen (2009), Simultaneous measurements of formaldehyde and nitrous acid in dew and gas phase in the atmosphere of Santiago, Chile, *Atmospheric Environment*, 43(38), 6106-6109.
- Sander, R. (2015), Compilation of Henry's law constants (version 4.0) for water as solvent, *Atmospheric Chemistry and Physics*, 15(8), 4399-4981.
- Seinfeld, J. H., and S. N. Pandis (2006), *Atmospheric chemistry and physics: from air pollution to climate change*, edited, John Wiley & Sons, Inc., New Jersey, USA.
- Young, A. H., W. C. Keene, A. A. P. Pszenny, R. Sander, J. A. Thornton, T. P. Riedel, and J. R. Maben (2013), Phase partitioning of soluble trace gases with size-resolved aerosols in near-surface continental air over northern Colorado, USA, during winter, *Journal of Geophysical Research: Atmospheres*, 118(16), 9414-9427.